Analyst

PAPER

View Article Online
View Journal | View Issue

Cite this: *Analyst*, 2014, **139**, 3895

Detection of polynucleotide kinase activity by using a gold electrode modified with magnetic microspheres coated with titanium dioxide nanoparticles and a DNA dendrimer†

Guangfeng Wang,*[ab] Ling Chen,[ab] Xiuping He,[ab] Yanhong Zhu[ab] and Xiaojun Zhang*[ab]

Received 18th March 2014
Accepted 11th April 2014

DOI: 10.1039/c4an00499j

www.rsc.org/analyst

In this paper, we have designed a signal amplified method for the electrochemical determination of polynucleotide kinase activity. It is based on (a) the peroxidase-like activity of magnetite microspheres (MNPs), (b) the specific recognition capabilities of titanium dioxide (TiO_2) with the phosphate groups of the capture probe and (c) the DNA dendrimer structure for signal amplification. MNPs coated with TiO_2 (TMNPs) were prepared and characterized by scanning electron microscopy (SEM) and Fourier transform infrared (FTIR) spectroscopy. TMNP–DNA dendrimers were formed by the hybridization of captured nucleic acids with a link probe. Cyclic voltammetry (CV) and electrochemical impedance spectroscopy (EIS) were carried out to study the electrocatalytic process. The formation of the TMNP–DNA dendrimer structures was related to the phosphorylated capture probe and further to the activity of polynucleotide kinase, which was the base of the polynucleotide kinase detection. The TMNP–DNA dendrimer based biosensor showed sensitive detection of polynucleotide kinase with a satisfying result; a low detection of 0.003 U mL^{-1} and wide linear range of 0.01 to 30 U mL^{-1} were achieved. Additionally, the present TMNP–DNA dendrimer based biosensor also demonstrated excellent selectivity, stability and reproducibility.

1. Introduction

As one of the most exciting biopolymers, DNA is no longer confined to its local role as the carrier of genetic information, due to its development in science.[1] It has showed great importance for its applications in nanotechnology,[2] materials science,[3] molecular computing[4] and (bio)analysis.[5] Since the duplex DNA structure based on the Watson–Crick complementarity of A–T and C–G base pairs was reported in 1965,[6] varieties of DNA structures have been studied successively such as intramolecular or intermolecular G-quadruplex or C-quadruplex (imotif) structures by the assembly of G-rich or C-rich DNA strands,[7] T–Hg^{2+}–T or C–Ag^{+}–C based supramolecular DNA nanostructures[8] and new ligandosides with artificial heterocycles in the DNA scaffold.[9] The diversity of structural patterns of DNA, together with the automated synthesis of the biopolymer, establishes a unique building block for the programmed assembly of nanostructures.[10] Indeed, ingenious 2D and 3D structures have been reported in recent years using the information encoded in the base sequence of nucleic acids.[11,12] 3D DNA structures have attracted great attention due to their unique advantages such as the ordered structure, spatial controllability, high stability, resistance to nonspecific protein adsorption, strong nucleic acid binding capacity and near natural conformation.[13] Dendrimers are monodispersed, three dimensional, hyperbranched, nanoscale polymeric architectures[14] which have been developed over several decades from being theoretically proposed and then further advanced.[15] Recently 3D DNA dendrimers have been studied[16] due to their high density,[17] enhanced physical, chemical, or biological activities,[18,19] controllable size,[20] and high efficiency for drug delivery and gene therapy.[20,21] Additionally, they have numerous functionalized groups which are beneficial for signal amplification.[22–24] Thus, it's promising to develop 3D DNA dendrimer based biosensors with signal amplification.

For the past few years, in numerous different explorations, metal nanoparticles,[25,26] which were used as catalytic labels for amplifying DNA-sensing or aptamer-sensing events, have been implemented in the development of field-effect transistors,[27] and electrical,[28] optical,[29] as well as microgravimetric nucleic

[a]*Anhui Key Laboratory of Chem-Biosensing, College of Chemistry and Materials Science, Center for Nanoscience and Nanotechnology, Anhui Normal University, Wuhu, 241000, P.R. China. E-mail: xjzhang@mail.ahnu.edu.cn; wangyuz@mail.ahnu.edu.cn*

[b]*State Key Laboratory of Chemo/Biosensing and Chemometrics, Hunan University, Changsha, 410082, P.R. China*

† Electronic supplementary information (ESI) available. See DOI: 10.1039/c4an00499j

acid-based biosensors.[27] Among known interesting nanomaterials used for a wide range of technological and biomedical applications, magnetic nanoparticles (such as Fe_3O_4) make a difference in separation techniques,[30] biological imaging,[31] and indeed in biological catalysis.[32] Magnetite microspheres (MNPs) possess a peroxidase-like activity, catalyzing the reduction of hydrogen peroxide resulting in a wide range of practical applications.[33–35] However, surface functionalization of MNPs is a necessary step for their application because it is an effective and necessary strategy to maintain chemical stability, to prevent the aggregation of MNPs and most importantly to make MNPs bear target specific ligands for further applications.[36] Thus MNPs coated or conjugated with other nanomaterials, catalysts or enzymes,[37,38] have attracted great attention, and these dual-functional nanoparticles could combine the properties of cores and shells commendably.[39] Nanostructured TiO_2, a distinguished semiconductor, has received much interest for its remarkable advantages, such as long term stability, multifunctionality, low cost and non-toxicity.[40] Specifically, TiO_2 can bind with phosphate groups on substrate peptides and proteins, on the basis of previous reports.[41–43]

In this paper, based on the specific binding capability of TiO_2 with phosphate groups,[41–43] prepared TiO_2-coated Fe_3O_4 magnetic nanoparticles were modified onto the 5′ end of phosphorylated DNA sequences, obtaining phosphorylated DNA–TMNP bioconjugates. With the help of a link probe, which was designed especially for hybridization with DNA–TMNPs, a DNA–TMNP dendrimer structure was fabricated on a gold electrode, resulting in an amplified electrochemical response based on the peroxidase-like TMNPs of the dendrimer system. As the biocatalytic response is closely related to the amount of phosphorylated capture probe, a convenient and reliable electrochemical biosensor with signal amplification based on a TMNP–DNA dendrimer structure has been fabricated.

2. Experimental

2.1. Chemicals and apparatus

HPLC-purified oligonucleotides (sequences are listed in Table S1 ESI†), were obtained from Sangon Biotechnology Co. Ltd. (Shanghai, China). T4 polynucleotide kinase (T4 PNK) (10 units per μL), Tris (hydroxymethyl) aminomethane (Tris), adenosine triphosphate (ATP) and other reagents were obtained from Sinopharm Chemical Reagent Co. Ltd. (Shanghai, China). All solutions were prepared with ultrapure water (18.2 MΩ cm) processed by PSDK2-10-C (Beijing, China). To test the practicality of the proposed sensor, human serum samples were collected as an example. Human serum samples were kindly obtained from the Yijishan Hospital (Wuhu, China). Before use, the human serum samples were centrifuged at 10 000 rpm for 15 min, and following this, the supernatant was diluted with Tris–HCl.

SEM images of the prepared composites were obtained using a Hitachi S-4800 scanning electron microscope (operated at 10 kV). Centrifugation was performed using a HERMLEZ 36 HK apparatus (Wehingen, Germany). The pH values of the PBS and Tris–HCl were measured with a glass electrode connected to a PHS-3C pH meter (Shanghai, China). FTIR spectra were measured on a FTIR-8400S spectrometer in the 300–2000 cm^{-1} region using powdered sample on a KBr plate (Japan, Shimadzu). Electrochemical measurements were performed using a model CHI660B electrochemical analyzer (ChenHua Instruments Co. Ltd., Shanghai, China) controlled by a personal computer with a bare or modified gold electrode (GE) (2 mm diameter) as the working electrode, a platinum wire as the auxiliary electrode, and a saturated calomel electrode (SCE) as the reference electrode.

2.2. Preparation of TiO_2-coated Fe_3O_4 nanocomposites

We first synthesized Fe_3O_4 microspheres according to the literature.[44] First, $FeCl_3 \cdot 6H_2O$ (1.35 g, 5 mmol) was dissolved in ethylene glycol (40 mL) to form a clear solution, followed by the addition of NaAc (3.6 g) and polyethylene glycol (1.0 g). After that, the mixture was stirred vigorously for 30 min and then sealed in a teflon-lined stainless-steel autoclave (50 mL capacity). Then, the autoclave was heated and maintained at 200 °C for 6–8 h, and allowed to cool at room temperature. Finally, the black products were washed several times with ethanol and dried at 60 °C for 6 h.

TiO_2-coated Fe_3O_4 magnetic nanocomposites were prepared by hydrolysis of tetrabutyl titanate [Ti $(OC_4H_9)_4$, TBOT] on the surface of magnetic Fe_3O_4 microspheres.[45] In short, the obtained MNPs were dispersed in 40 mL of absolute alcohol and stirred for half an hour, followed by the slow addition of 0.5 mL of TBOT. Then 0.05 mL glacial acetic acid was added into the mixture gradually with vigorous stirring for 2 to 4 h to control the hydrolysis reaction. When a milky white suspension was observed after magnetic separation of the MNPs onto the wall of the tube, the as-prepared TMNPs were isolated, taken out, washed repeatedly with ethanol, and allowed to dry naturally. Then the TMNPs were annealed at 400 °C for 2 h and finally dispersed in absolute ethyl alcohol before analytical use.

2.3. Preparation of phosphorylated DNA–TMNP bioconjugates

Phosphorylated DNA–TMNP bioconjugates were prepared, starting with the formation of phosphorylated S2, which is involved in the following steps. 30 U mL^{-1} T4 PNK, in the presence of ATP, was introduced as a culture solution containing 3 μM capture probe S2. Hence, the phosphorylation sites on the phosphorylated peptides were introduced at the 5′ termini of the S2. After incubating for 5 h, modification of the TMNPs on the phosphorylated S2 (P–S2) was carried out by incubating P–S2 with 55 ng mL^{-1} TMNP solution for 3 h at room temperature to capture the P–S2 on the TMNPs based on the specific adsorption of the phosphorylation sites and Ti^{4+},[41–43] and linkage between P–S2 and the TMNPs (P–S2–TMNPs) was processed. With different concentrations of T4 PNK for phosphorylation, the related amounts of P–S2–TMNPs were obtained. The P–S2–TMNPs were washed three times with Tris–HCl buffer and finally collected *via* magnetic separation for further use.

2.4. Self-assembly of the substrate probe on a gold electrode

Before use, oligonucleotides were dissolved in 0.05 M Tris–HCl buffer (pH 7.4) and stored at 4 °C for one night. Then the oligonucleotide solutions were heated to 80 °C and slowly cooled to room temperature. Prior to modification, the gold electrode was first pretreated according to the following methods. The gold electrode was first polished with 0.3 and 0.05 mm alumina powder, and then sonicated in ethanol and ultrapure water for 5 min, respectively. After that, to remove any remaining impurities *via* electrochemical cleaning, the gold electrode was scanned in 0.1 M H_2SO_4 between −0.2 and 1.55 V at 100 mV s^{-1} until a steady-state redox wave was observed. The immobilization of the substrate probe (S1) was performed by dropping 30 μL of 0.05 M Tris–HCl buffer (pH 7.4) containing 1.0 μM thiolated nucleic acid S1 probe and 100 mM NaCl onto the cleaned gold electrode in a humidified chamber for 10 h. The self-assembly proceeded through covalent bond formation between the thiol of S1 and the Au atom (Au–S bond). Then the gold electrode was rinsed with water and incubated in 2 mM 6-mercaptohexanol in Tris–HCl buffer for 2 h to eliminate the nonspecific-bonded probe. After being rinsed thoroughly with the washing buffer (10 mM PBS, pH 7.4, 100 mM NaCl), the S1 probe modified gold electrode (S1/GE) was prepared and stored at 4 °C in PBS (10 mM, pH 7.4).

2.5. Preparation of the TMNP–DNA dendrimer based biosensor

The prepared S1/GE was incubated in the hybridization buffer, 0.05 M Tris–HCl buffer (pH 7.4) containing magnetically separated P–S2–TMNPs and 3 μM link probe, S3 (which played a role in connecting P–S2–TMNPs), at 35 °C to form the TMNP–DNA dendrimer structure modified electrode (regarded as S3–P–S2–TMNPs–S1/GE). After incubation for 5 h, the modified electrode was washed with water thoroughly and dried using nitrogen before electrochemical measurements. To certify the formation of the TMNP–DNA dendrimer, contrast experiments were performed to investigate the activity of the TMNP–DNA dendrimer structure modified electrode; when S1/GE was only hybridized with P–S2–TMNPs, the obtained electrode was named P–S2–TMNP–S1/GE. Additionally, we studied a modified electrode on which S1/GE was hybridized with S3 and P–S2 in the absence of TMNPs, resulting in S3–P–S2–S1/GE.

2.6. The electrochemical experimental process

All of the electrochemical experiments were carried out at room temperature. Cyclic voltammetry (CV) was performed in 0.05 M Tris–HCl (pH 7.4) within the potential range from 0.4 to −0.4 V using a step potential of 0.05 V at a scan rate of 50 mV s^{-1}. Electrochemical impedance spectroscopy (EIS) was performed in 1/15 M PBS (pH 7.4) containing 5 mM $Fe(CN)_6^{3-}/Fe(CN)_6^{4-}$ and 0.1 M KCl in the frequency range from 0.1 Hz to 100 kHz with 5 mV as the amplitude at a polarization potential of −0.18 V. The amperometric current was also measured at −0.2 V in Tris–HCl (0.05 M, pH 7.4) with the addition of H_2O_2 as the sensor rotated at 3000 rpm for optimum sensitivity. Detection of T4 PNK activity was performed by incubating the S1/GE in Tris–HCl (0.05 M, pH 7.4) containing the processed P–S2–TMNPs which were captured by various quantities of P–S2 associated with different concentrations of T4 PNK and 3 μM S3. All of the electrochemical experiments were carried out at room temperature.

3. Results and discussion

3.1. The configuration of the system

Scheme 1 outlines the fabrication of the TMNP–DNA dendrimer based biosensor for the investigation of T4 PNK activity. First, TMNPs were attached to phosphorylated S2 by the specific recognition of Ti^{4+} in TMNPs with kinase induced phosphopeptides,[41–43] obtaining P–S2–TMNPs. Then the S1/GE hybridized with the P–S2–TMNPs by 15 bases at the 3′ end of S2 to form the TMNP–DNA complex on the electrode in the presence of link probe, S3, which has 15 complementary base pairs at its two ends with S2. S3 hybridizes with the P–S2–TMNPs and the chain hybridization is triggered, resulting in the formation of the TMNP–DNA dendrimer on the electrode. Therefore, a mass of TMNPs were encapsulated into the TMNP–DNA dendrimer based structure. The electrochemical T4 PNK sensing strategy occurs as indicated by the enzyme mimetic activity of MNPs[33–35] in TMNPs. Based on the bioelectrocatalyzing reduction of H_2O_2 by TMNPs, detection of T4 PNK activity was achieved in which the electrochemical signal may have been amplified by the dendrimer structure.

3.2. Characterization

3.2.1. SEM and FTIR characterization. The characterization of MNPs and TMNPs was implemented by means of typical SEM, as well as FTIR spectroscopy. The SEM images of different magnifications in Fig. 1A(a and b) show that the MNPs were prepared successfully with high size uniformity and an average diameter of ~0.255 μm. After the surfaces of the MNPs were

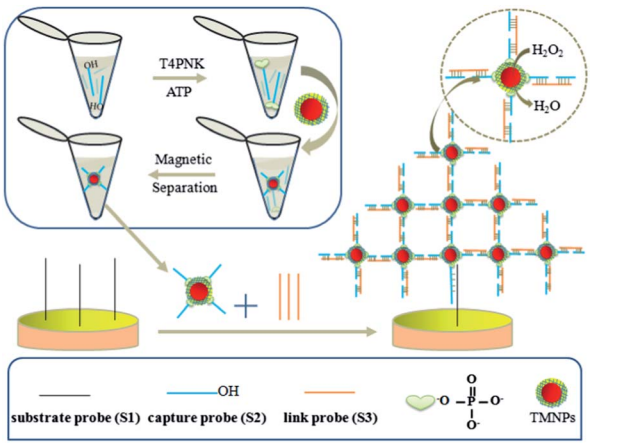

Scheme 1 Fabrication of the TMNP–DNA dendrimer biosensor and the electrochemical catalysis process based on TMNPs.

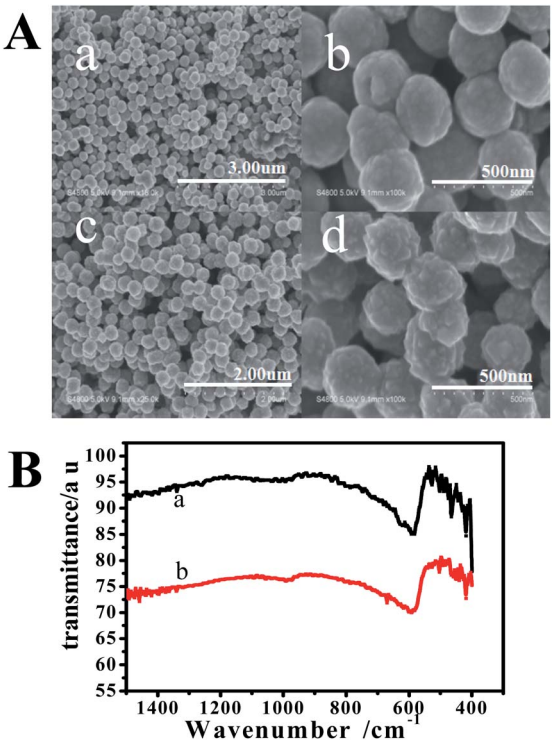

Fig. 1 (A) Low magnification (a) and high magnification (b) SEM images of the prepared MNPs, and low magnification (c) and high magnification (d) SEM images of the prepared TMNPs; (B) FTIR spectra of the MNPs (curve a) and TMNPs (curve b).

modified with TiO_2, and from the SEM images of different magnifications shown in Fig. 1A(c and d), we can see a roughened layer on the surface of the MNPs clearly. The FTIR spectra of the MNPs and TMNPs are shown in Fig. 1B. The absorption band at around 580 cm^{-1} is attributed to the Fe–O stretch shown as curve a of Fig. 1B. After surface modification of TiO_2, as shown in curve b of Fig. 1B, the absorption band at around 580 cm^{-1} is a little augmented because of the Ti–O stretch and Fe–O stretch.[46,47]

3.2.2. EIS characterization. As electrochemical impedance spectroscopy is an effective method for probing the features of surface modified electrodes,[48,49] EIS measurements were performed to study the modified electrodes with different interfacial processes. R_{et} indicates the surface electron transfer electrical resistance of the electrode. Fig. 2A shows the impedance spectra of different electrodes with different modification processes, which were obtained in the form of a Nyquist plot. The bare gold electrode shows a definite small semicircular domain (curve a), illustrating a very low electron transfer resistance. The R_{et} rises obviously for S1/GE (curve b) due to the fact that the capture sequence can severely hinder the electron transfer toward the electrode surface. Then the obtained P–S2–TMNPs–S1/GE was also studied, resulting in the diameter of the semicircle shown as curve c of Fig. 2A being slightly larger than that of curve b. As shown in curve d of Fig. 2A, after S1/GE hybridizing with P–S2–TMNPs and S3 to obtain S3–P–S2–TMNP–S1/GE, the diameter of the semicircle increases greatly because of the increase in electron transfer resistance on the electrode, demonstrating that the TMNP–DNA dendrimer structure was likely formed on the electrode as we predicted before. All of these results indicate the possibility of the TMNP–DNA dendrimer in curve d.

We also studied the cyclic voltammetric response of different modified electrodes to investigate our proposal. As shown in curve a of Fig. 2B, a negligible CV signal is obtained in Tris–HCl (pH 7.4) with 100 μM H_2O_2 on a bare or S1 modified GE, demonstrating that there is no catalytic activity toward hydrogen peroxide on a bare GE or S1/GE (curve a and b of Fig. 2B). After incubating S1/GE with S2 alone (curve c of Fig. 2B), no obvious change is found in the CV response, implying that S2 DNA strands on the electrode surface cannot catalyze H_2O_2. However, if the bare electrode is incubated with S1, P–S2–TMNPs and S3 together, as shown in curve e of Fig. 2B, a large electrocatalytic response is obtained on S3–P–S2–TMNP–S1/GE, indicating that the proposed sensor has an effective response to hydrogen peroxide because of the intrinsic enzyme mimetic activity of TMNPs loaded on the electrode surface successfully. To confirm this, a control experiment was carried out by incubating S1/GE with S3 and P–S2 without TMNPs. No obvious change is found in the CV response (curve d of Fig. 2B), implying that the system does not have the ability to catalyze H_2O_2 in the absence of TMNPs. Based on the cyclic voltammetric results in Fig. 2B, the TMNP–DNA dendrimer based biosensor was further studied for its response toward different concentrations of H_2O_2, as shown in Fig. S1 ESI.†

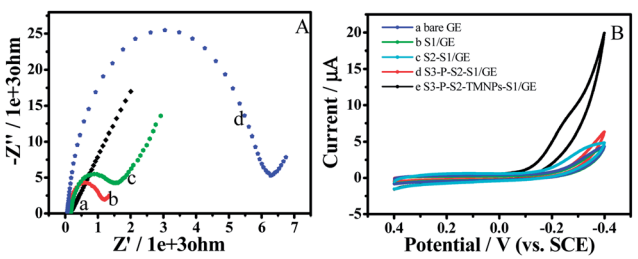

Fig. 2 (A) EIS results of the electrodes after different modification procedures: a bare GE (a), S1/GE (b), P–S2–TMNP–S1/GE (c), S3–P–S2–TMNP–S2/GE (d); (B) cyclic voltammograms of bare GE (a), S1/GE (b), S2–S1/GE (c), S3–P–S2–S1/GE (d), S3–P–S2–TMNP–S1/GE (e) in Tris–HCl (pH 7.4) with 100 μM H_2O_2.

3.3. Detection of T4 PNK activity

After discussing optimization conditions and the effect of the TMNP–DNA dendrimer structure for electrochemical amplification (the details are shown in Fig. S2 and S3 ESI,† respectively), we further study the response of the system in relation to the concentration of T4 PNK based on the TMNP–DNA dendrimer biosensor. As Fig. 3A shows, a series of dynamically increased CV peak currents in response to T4 PNK with increasing concentrations were observed distinctly. Fig. 3B is the amperometric current which reaches a steady state response rapidly with each addition of 100 μM H_2O_2. Fig. 3C depicts the resulting calibration curve of the current *vs.* the logarithm of the

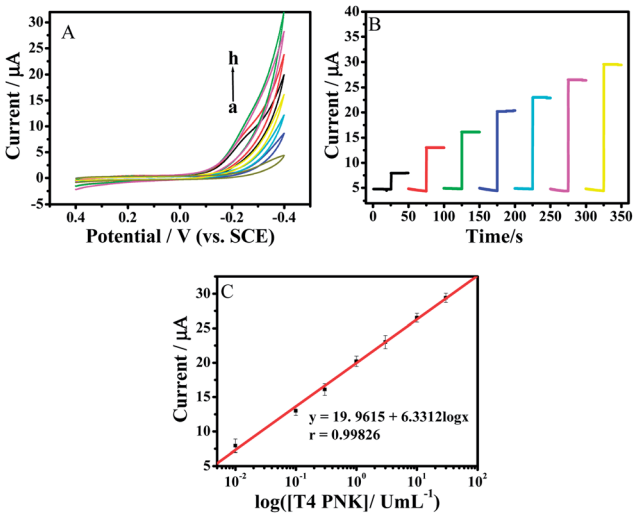

Fig. 3 (A) CV results and (B) the steady state amperometric current at −0.4 V on S3–P–S2–TMNP–S1/GE in the presence of various concentrations of T4 PNK (a–h): 0, 0.01, 0.1, 0.3, 1, 3, 10, 30 U mL^{-1} in Tris–HCl (pH 7.4) with 100 μM H_2O_2; (C) the corresponding calibration curve of current *vs.* the concentration of T4 PNK.

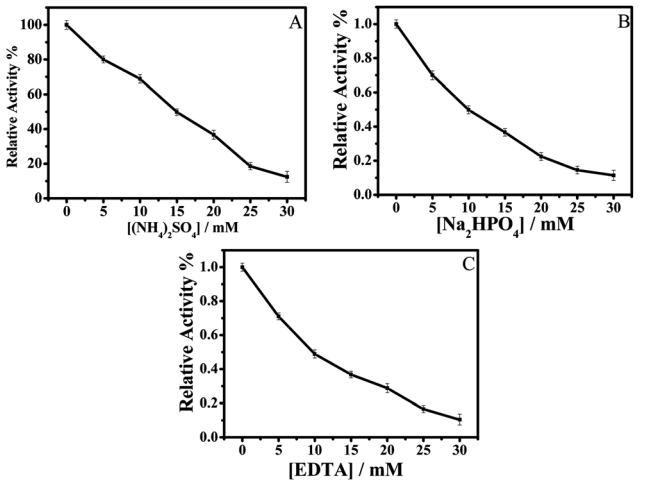

Fig. 4 Inhibitive effects of (A) $(NH_4)_2SO_4$, (B) Na_2HPO_4, and (C) EDTA on phosphorylation at S3–P–S2–TMNP–S1/GE. The assays were carried out in 0.05 M Tris–HCl buffer (pH 7.4), containing 30 U mL^{-1} T4 PNK.

T4 PNK concentration between 0 and 30 U mL^{-1}. A detection limit of T4 PNK was calculated to be 0.003 U mL^{-1} (evaluated using a signal three-fold the background noise). The resulting sensitivity originates from the amplification path provided by the biocatalytic system. The relative standard deviation (RSD) for 3 successive determinations was 2.98%, suggesting a good stability and reproducibility. In addition, the practicality of the proposed strategy was also investigated by the detection of T4 PNK in 100-fold diluted human serum samples and the detection procedure was the same as that described in the aforementioned experiment for T4 PNK detection in clean Tris–HCl buffer solution. As can be seen from Table S2 ESI,† the results of the application are satisfactory.

3.4. Inhibition investigation

In order to evaluate the inhibitory effects on T4 PNK activity, we studied the validity of T4 PNK with its inhibitors at various concentrations in the reaction buffer, such as $(NH_4)_2SO_4$, Na_2HPO_4 and EDTA. The bioelectrocatalysis signal of S3–P–S2–TMNP–S1/GE was considered as i_0, and the response of S3–P–S2–TMNP–S1/GE dealing with $(NH_4)_2SO_4$ or other inhibitors was regarded as i, then i/i_0 was stated as the relative activity. From Fig. 4, it was obvious that the relative activity decreased gradually with the concentration of inhibitors, implying that the validity of T4 PNK was restrained by these three inhibitors. According to previous reported research, the effect of these inhibitors on the phosphorylation reaction can be explained in two possible points. On the one hand, a high concentration of salts probably inhibit the activity of DNA on the 5′-hydroxyl group. On the other hand, the high concentration of salts may also significantly affect the conformation of the enzyme, resulting in further inhibitive effects on the activity of PNK and the affinity between substrates and its kinase.[50]

4. Conclusions

In summary, this work describes a novel electrochemical biosensor, which is based on the specific recognition of TiO_2 for kinase-induced phosphopeptides and the peroxidase-like catalysis activity of MNPs. It is an ingenious strategy that combines TMNP–DNA dendrimer structure amplification with the peroxidase-like activity of MNPs on H_2O_2. Considering the high sensitivity and selectivity of this kind of dendrimer amplified biosensor, it is expected to achieve great access to applications involving real samples. Furthermore, alternative sensing devices can also be envisaged for indirect detection of other metal ions or proteins based on this amplified dendrimer structure (*e.g.*, Ag^+ by cytosine, Hg^{2+} by thymine, and target molecules by aptamers).

Acknowledgements

This work was financially supported by the projects (21073001, 21005001 and 21371007) from National Natural Science Foundation of China, Anhui Provincial Natural Science Foundation (1208085QB28), Anhui Provincial Natural Science Foundation for Distinguished Youth (1408085J03), Natural Science Foundation of Anhui (KJ2012A139) and the Program for Innovative Research Team at Anhui Normal University.

Notes and references

1 E. T. Kool, *Acc. Chem. Res.*, 2002, **35**, 936.
2 H. Yan, X. Zhang, Z. Shen and N. C. Seeman, *Nature*, 2002, **415**, 62.
3 E. G. Hvastkovs and D. A. Buttry, *Analyst*, 2010, **135**, 1817.
4 Y. Benenson, T. Paz-Elizur, R. Adar, E. Keinan, Z. Livneh and E. Shapiro, *Nature*, 2001, **414**, 430.
5 W. J. Ansorge, *New Biotechnol.*, 2009, **25**, 195.

6 J. D. Watson and F. H. C. Crick, *Nature*, 1953, **171**, 737.
7 A. T. Phan, M. Gueron and J. L. Leroy, *J. Mol. Biol.*, 2000, **299**, 123.
8 A. Ono, S. Cao, H. Togashi, M. Tashiro, T. Fujimoto, T. Machinami, S. Oda, Y. Miyake, I. Okamoto and Y. Tanaka, *Chem. Commun.*, 2008, 4825.
9 A. Fu, C. Micheel, J. Cha, H. Chang, H. Yang and A. P. Alivisatos, *J. Am. Chem. Soc.*, 2004, **126**, 10832.
10 K. V. Gothelf and T. H. LaBean, *Org. Biomol. Chem.*, 2005, **3**, 4023.
11 P. K. Lo, K. L. Metera and H. F. Sleiman, *Curr. Opin. Chem. Biol.*, 2010, **14**, 597.
12 D. Astruc, E. Boisselier and C. Ornelas, *Chem. Rev.*, 2010, **110**, 1857.
13 Y. Cheng, L. Zhao, Y. Li and T. Xu, *Chem. Soc. Rev.*, 2011, **40**, 2673.
14 C. Lin, Y. Liu, S. Rinker and H. Yan, *ChemPhysChem*, 2006, **7**, 1641.
15 C. J. Hawker and J. M. J. Frechet, *J. Am. Chem. Soc.*, 1990, **112**, 7638.
16 R. J. Amir, E. Danieli and D. Shabat, *Chem.–Eur. J.*, 2007, **13**, 812.
17 M. Najlah, S. Freeman, D. Attwood and A. D'Emanuele, *Int. J. Pharm.*, 2006, **308**, 175.
18 D. Li, Y. Yan, A. Wieckowska and I. Willner, *Chem. Commun.*, 2007, 3544.
19 U. Boas and P. M. H. Heegaard, *Chem. Soc. Rev.*, 2004, **33**, 43.
20 A. M. Caminade, P. Servin, R. Laurent and J. P. Majoral, *Chem. Soc. Rev.*, 2008, **37**, 56.
21 D. A. Tomalia, *Science*, 1991, **252**, 1231.
22 E. Sella and D. Shabat, *J. Am. Chem. Soc.*, 2009, **131**, 9934.
23 Y. H. Sun, R. M. Kong, D. Q. Lu, X. B. Zhang, H. M. Meng, W. H. Tan, G. L. Shen and R. Q. Yu, *Chem. Commun.*, 2011, **47**, 3840.
24 G. J. Li, X. L. Li, J. Wan and S. S. Zhang, *Biosens. Bioelectron.*, 2009, **24**, 3281.
25 R. Polsky, R. Gill, L. Kaganovsky and I. Willner, *Anal. Chem.*, 2006, **78**, 2268.
26 J. Wang, D. Xu, A. N. Kawde and R. Polsky, *Anal. Chem.*, 2001, **73**, 5576.
27 E. Sharon, R. Freeman, R. Tel-Vered and I. Willner, *Electroanalysis*, 2009, **21**, 1291.
28 J. Wang, G. Liu and A. Merkoci, *J. Am. Chem. Soc.*, 2003, **125**, 3214.
29 R. Gill, M. Zayats and I. Willner, *Angew. Chem.*, 2008, **120**, 7714.
30 H. H. Yang, S. Q. Zhang, X. L. Chen, Z. X. Zhuang, J. G. Xu and X. R. Wang, *Anal. Chem.*, 2004, **76**, 1316.
31 M. Brähler, R. Georgieva, N. Buske, A. Müller, S. Müller, J. Pinkernelle, U. Teichgräber, A. Voigt and H. Bäumler, *Nano Lett.*, 2006, **6**, 2505.
32 H. H. Yang, S. Q. Zhang, X. L. Chen, Z. X. Zhuang, J. G. Xu and X. R. Wang, *Anal. Chem.*, 2004, **76**, 1316.
33 N. Ding, N. Yan, C. Ren and X. Chen, *Anal. Chem.*, 2010, **82**, 5897.
34 L. Z. Gao, J. Zhuang, L. Nie, J. B. Zhang and Y. Zhang, *Nat. Nanotechnol.*, 2007, **2**, 577.
35 H. Wei and E. K. Wang, *Anal. Chem.*, 2008, **80**, 2250.
36 Y. Pan, X. W. Du, F. Zhao and B. Xu, *Chem. Soc. Rev.*, 2012, **41**, 2912.
37 P. D. Stevens, J. Fan, H. M. R. Gardimalla, M. Yen and Y. Gao, *Org. Lett.*, 2005, **7**, 2085.
38 S. C. Tsang, V. Caps, I. Paraskevas, D. Chadwick and D. Thompsett, *Angew. Chem., Int. Ed.*, 2004, **43**, 5645.
39 K. C. F. Leung, S. H. Xuan, X. M. Zhu, D. W. Wang, C. P. Chak, S. F. Lee and K. W. H. Watson, *Chem. Soc. Rev.*, 2012, **5**, 1911.
40 Z. Su and W. Zhou, *J. Mater. Chem.*, 2011, **21**, 8955.
41 L. Qiao, C. Roussel, J. J. Wan, P. Y. Yang, H. H. Girault and B. H. Liu, *J. Proteome Res.*, 2007, **6**, 4763.
42 J. Ji, H. Yang, Y. Liu, H. Chen, J. Kong and B. Liu, *Chem. Commun.*, 2009, 1508.
43 S. M. Wang, P. Su, J. Huang, J. W. Wu and Y. Yang, *J. Mater. Chem. B*, 2013, **1**, 1749.
44 H. Deng, X. L. Li, Q. Peng, X. Wang, J. P. Chen and Y. D. Li, *Angew. Chem., Int. Ed.*, 2005, **18**, 2842.
45 J. Bai, Y. J. Zhao, Z. B. Wang, C. H. Liu, Y. C. Wang and Z. P. Li, *Anal. Chem.*, 2013, **85**, 4813.
46 J. Madejová, *Vib. Spectrosc.*, 2003, **31**, 1.
47 Y. H. Yan, Z. F. Zheng, C. H. Deng, X. M. Zhang and P. Y. Yang, *Chem. Commun.*, 2013, **49**, 5055.
48 E. Katz and I. Willne, *Electroanalysis*, 2003, **15**, 913.
49 S. Dong, G. Luo, J. Feng, Q. W. Li and H. Gao, *Electroanalysis*, 2001, **13**, 30.
50 Y. H. Wang, X. X. He, K. M. Wang, X. Q. Ni, J. Su and Z. F. Chen, *Biosens. Bioelectron.*, 2012, **32**, 213.

